Vietnam Journal of Catalysis and Adsorption
Tạp chí xúc tác và hấp phụ Việt Nam

https://jca.edu.vn

Evaluating the corrosion resistance of Aluminum alloy A6063 with and without protective coatings in a simulated environment proton exchange membrane fuel cells

Anh Tuyet Thi Ngo[1,*], Linh Do Chi[1], Hanh Hong Pham[1], Hoa Bui Thi[1], Thai Hong Giang[1], Lam Duc Nguyen[1], San Pham Thy[1]

[1] *Lab. of Technologies for Hydrogen and Corrosion, Institute of Materials Science, Viet Nam Academy of Science and Technology, 18 Hoang Quoc Viet, Ha Noi, Viet Nam*
** Email: tuyetnta@ims.vast.ac.vn*

ARTICLE INFO

Received: 30/03/2024
Accepted: 02/07/2024
Published: 30/12/2024

Keywords:
Aluminum alloy A6063;
Corrosion behavior;
PEFCs; EIS; protective coatings

ABSTRACT

In this study, Ni-coating and Au/Ni-coating were preparated by electroplating method at room temperature (25^0 C) and 45^0 C with various plating time on A6063 alloy substrate. The corrosion behavior of A6063 with and without protective coatings (Ni-coating and Au/Ni-coating) were evaluated in a solution simulating environment of Proton exchange membrane fuel cells (PEMFCs), 0.5 M H_2SO_4 and 200 ppm HF at temperatures 60 ^{0}C. Electrochemical techniques including polarization tests and impedance spectrum are used to evaluate corrosion behaviour. The surface and cross-section morphology, the chemical composition of the specimens were characterized by scanning electron microscope (SEM) and energy-dispersive X-ray (EDS) The results shown that corrosion resistance of specimens coated at room temperature was better than those coated at 45^0C. Aluminum alloy A6063 with protective coatings significantly improved the corrosion resistance in a simulated environment proton exchange membrane fuel. While, the corrosion current density of the Au/Ni-coating reduced by 6.4 times compared to the Ni-coating and 33.9 times compared to the A6063 without coating.

Introduction

Fuel cells (FCs) are electrochemical devices that directly convert chemical energy from fuel into electricity, heat, and H_2O [1]. These electrochemical devices can operate as long as fuel (mainly hydrogen) and an oxidant (O_2) are supplied [2,3]. Proton exchange membrane fuel cells, or PEMFCs, temperature of operation range 30–80 °C [1]. In fact, the temperature effects on performance and reliability are one of important issues. When chemical reactions occur and transport of charges begins, heat is generated in the cells and temperature rises. The elevated temperature increases the rate of chemical reaction and water activity that affects transport of charges and reactants. When loads for the stack continuously change, the temperature profile in the stack varies and the limit set can be exceeded. In addition to the temperature effects on reliability of membranes and catalysts. A high working temperature at a given current load increases water flux in the membrane from the anode to the cathode and likely causes dehydration. The rate of Pt particle size growth gets larger at elevated temperature and resulting loss of platinum surface area

https://doi.org/10.62239/jca.2024.067

causes efficiency degradation. Therefore, management of temperature by controlling the coolant flow plays an important role in ensuring highly reliable and efficient operations and properties of components of the fuel cell system [4]. Too high or too low temperature and humidity have a direct impact on the performance of the membrane and stack. In order to improve gross efficiency and simplify fuel cell design, work has been undertaken in the past few decades to employ different techniques such as air-cooled PEM fuel cells and stacks[1], cooling with heat spreaders[5], cooling with liquid[6]…The cooling system design has a direct impact in meeting the durability, cost, and performance targets for commercialization [5,6]. Among many cooling with heat spreaders materials, aluminium is one of the most interesting because is unlimitedly recyclable and is widely used for the manufacture throughout the world [7]. A6063 is normally used for cooling plate because of its outstanding advantages such as: low cost, high corrosion resistance, and easy to modify the surface [8]. However, in Acidic environments of a simulated environment proton exchange membrane fuel cells containing halogens like fluoride, aluminium alloys are susceptible to corrosion, impelling the need for corrosion protection by means of surface treatment/modification or protective coatings [9]. Nickel is the best performing alloys in corrosion, high and low temperature resistance, with good ductility and toughness. Nickel plating is used as well for aesthetic purposes since the resulting coatings are very shiny and durable. However, in some cases where materials are used in harsh environments, an additional on layer of gold or platinum plating is demaned to protect against corrosion. In this study, protective coatings consist a Nikel coating and a Nikel coating add a gold coating on A6063 were performed by electroplating method. The corrosion resistance of Aluminum alloy A6063 with and without protective coatings in a simulated environment proton exchange membrane fuel cells was evaluated.

Experimental

Material preparation

The aluminium alloy A6063 was used as a substrate and machined into plates with dimension of 50x50mm. After that, the specimens were polished using SiC papers with grit from #400 to #1200. Before the coating treatment, the surface of the specimens was removed grease, treated in Zincate bath and cleaned with deionized water.

The protective coatings were prepared by the electroplating method. Aluminium alloy A6063 was connected as a cathode (negative pole) and nikel plate as an anode (positive pole) in a two-electrode wiring system during the electroplating process. For Ni-electroplating, the chemical composition of the electrolyte bath solution consisted of 150 g/l $NiS0_4.7H_2O$, 150 g/l $Na_2SO_4.10H_20$, 50 g/l $MgSO_4.7H_20$, 25g/l H_3B0_3. This electrolyte has $NiSO_4$ $.7H_2O$, being the nickel ions (Ni^{2+}) main source, Na_2SO_4 and $MgSO_4$ increase the conductivity of the solution and H_3BO_3 role as an additive or adjusts the pH of the electroplating solution. Ni-coatings were performed at room temperature (25^0 C) and 45^0 C; cathode current density is 0.8 A/dm^2 and pH of solution of 4 for 20, 40, and 60 minutes, using a DC power source (IMS-CPR-02). Au/Ni-coatings were carried out in Au-electroplating with the chemical composition of the electrolyte for Au-electroplating bath solution consisted of 4 g/l $KAu(CN)_2$, 30g/l $C_6H_8O_7$, 50g/l $C_6H_5K_3O_7$, 3g/l $CoSO_4.7H_2O$ and by applied the samples which have a available intermediate Ni-coatings with electroplating time of 20 minutes, and continued Au-coated process in various time of 20 to 60 minutes, cathode current density is 0.6 A/dm^2. In which, $KAu(CN)_2$ is the gold ions (Au^{3+}) main source, $CoSO_4.7H_2O$ increase the conductivity of the solution and $C_6H_8O_7$, $C_6H_5K_3O_7$ acts as a complex. In the gold electroplating process, the anode is made of mixed metal oxide (MMO) and the cathode is an aluminum alloy A6063. At the end of this process, the samples were dried with a stream of air and cut in to discs with the size of Φ15×2 (mm) for specimen's characterization.

Electrochemical measurements and Static corrosion behavior

A polarization test and impedance spectrum were carried out for the aluminium alloy A6063 with and without The protective coatings in a solution of 0.5 M H_2SO_4 + 200 ppm HF at 60^0 C by a potentiostat (Autolab PGSTAT-302N, Metrohm/Netherlands). Specimens were trimmed to fix with a holder electrode with a diameter of 15 mm. A three electrodes cell was used in which the counter electrode was platinum and the reference electrode was saturated Ag/AgCl and a specimen was working electrode. The open circuit potential was measured for 600 s. Subsequently,

https://doi.org/10.62239/jca.2024.067

polarization curves was measured in the potential range from −0.25 V to +1.0 V vs. open circuit potential (Eocp) at a scan rate of 1 mV/s.

Static corrosion behavior was evaluated by immersion of samples in a solution of 0.5 M H_2SO_4 + 200 ppm HF at 60 ^{0}C for 45 days. After 7, 14, 30 and 45 days of immersion process, samples taken out, removed corrosion products, cleaned with distilled water, then dried in air at 100 ^{0}C for 4 hours, and finally weighed using the electronic scale (Ohaus PA214) with accuracy of 0.0001. The weight loss of the samples was used to calculate the corrosion rate of the samples.

Material characterization

The surface and cross-section morphology of the specimens were characterized by field-emission scanning electron microscope (FE-SEM; FEI, Quanta FEG250) equipped with an energy-dispersive X-ray spectrometer (EDS; EDS, EDAX).

Results and discussion

Microstructural of electroplating coatings on A6063 substrate

SEM images of surface of Ni- coatings with various plating times and temperatures are shown in Figure 1. The sample's surface morphology at room temperature and 45^{0}C, showed nearly no flaws and homogenous precipitated crystals arranged in a tile-roof stacked pattern after 20 minutes of plating time. Uneven crystal sizes with some defects were observed on the samples' surface with increasing plating time and temperature (Fig.1 b),(c),(e) and (f).

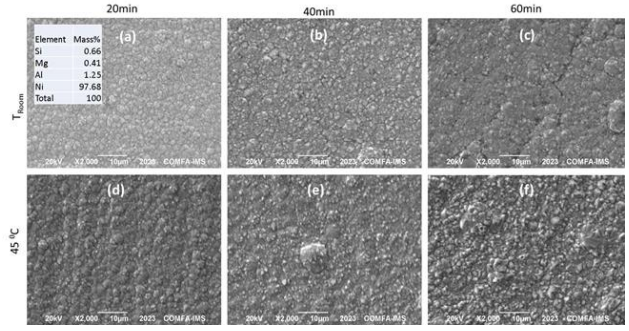

Fig. 1. SEM image of Ni-coatings

Furthermore, at the same of plating time, crystals with larger sizes are formed in a higher temperature. This could be as a result of the H_2 gas released during the plating process altering the crystal arrangement and the high temperature accelerated the Ni precipitation reaction on the sample surface. The results of EDS analysis on representative samples are also shown in Fig.1a. Accordingly, the amount of Ni > 90% shown that Ni element is the main component of electroplating coating.

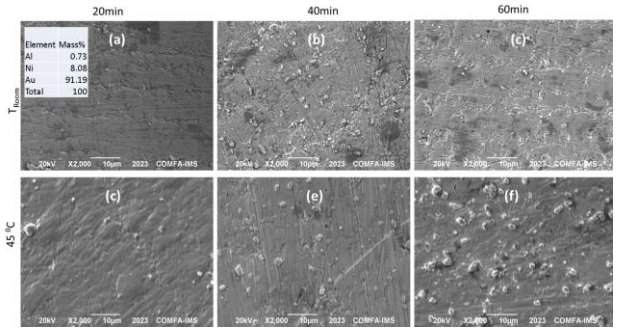

Fig. 2. SEM image of Au-coatings

The Figure 2 expressed SEM images of surface of Au/Ni-coatings. A fine grain crystalline structure on the surface was observed at 20 minutes of plating time. For 40 and 60 minutes of plating time samples, some larger-sized particles developed on the surface structure are clearly visible as shown in Figure 2(b),(c),(e) and (f). Especially at a temperature of 45^0 C and coating time of 60 minutes sample, many large particles grow on A6063 substrate, creating a rough surface. The thickness of coatings was determined by cross-sectional SEM image in Fig.3. In which, fig. 3(a), (b) and (c) represent cross-sectional SEM of Ni-coatings. The findings demonstrate that the thickness of the Ni-coating gradually increases with time. The thickness reached 7, ~9 and > 11 µm at 20 ,40 and 60 minutes of coating time, respectively. Fig 3 (d), (e) and (f) shown that Au/Ni-coating consist two layers with an outer thin Au-layer and inner layer which have a available intermediate Ni-coatings with electroplating time of 20 minutes.

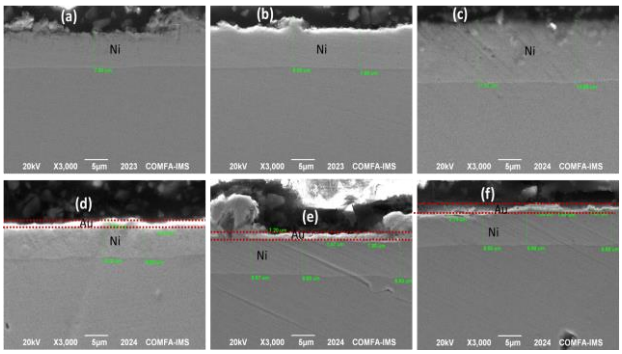

Fig. 3. SEM cross-section image of samples

The thickness of inner Ni-layer about 6.6 to 7 µm while, thickness of outer Au-layer reached 0.9, 1.2 and 1.5 µm at 20 ,40 and 60 minutes of coating time. The results

https://doi.org/10.62239/jca.2024.067

shown that the thickness of the inner Ni layer of Au/Ni-coating is nearly unaltered compared to the 20-minute Ni plating sample without Au-layer and the thickness of the Au layer increases with time. However, Au precipitated at a much slower rate than Ni. This is explained because the current efficiency of Ni-electroplating process is very high, usually reaching > 95%, while the Au-electroplating process has a lower current efficiency ~80% due to very low concentration of Au^{3+} in the electroplating solution and the rate of release reaction of H_2 is much higher than that in Ni-electroplating process.

Corrosion behavior of plating layer on A6063 substrate

Polarization behavior and EIS

Fig. 4a illustrates the polarization curves of the samples in a solution of 0.5 M H_2SO_4 + 200 ppm HF at 60° C. The corrosion potential (E_{corr}) and corrosion current density (i_{corr}) were determined using the Tafel extrapolation method with NOVA 1.10 software, and the corrosion rates (CR) were calculated from the polarization curves.

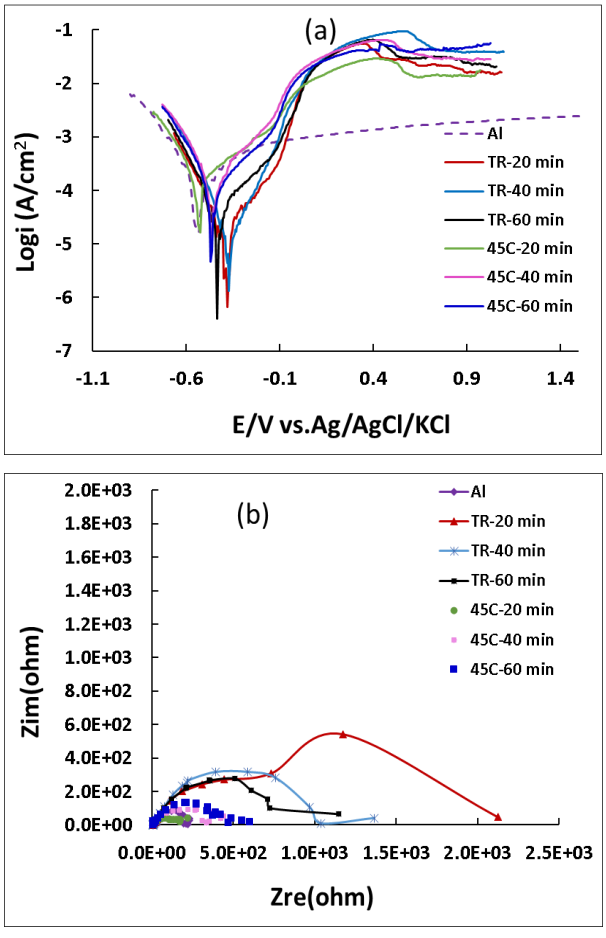

Fig 4. a-Polarization curves and b-EIS of Ni-coatings

The i_{corr} and E_{corr} value for the A6063 substrate are 51.28 μA/cm² and -560 mV. For specimens coated at different plating time and various temperature, the i_{corr} values are 9.77, 23.44, 22.39, 46.21, 33.22 and 34.19 μA/cm² and E_{corr} values are -382, -380, -432, -534, -457 and -488 mV for TR-20 min-, TR-40 min-, TR-60 min-, 45C-20 min-, 45C-40 min-, 45C-60 min-specimens, respectively. The E_{corr} of coated specimens shifted towards the positive direction. These results are consistent with previous investigations [17,18]. Additionaly, corrosion rate values of specimens shown that corrosion resistance of A6063 with an electroplating coating increased to 5.24 times compared to A6063 without an electroplating coating. These findings confirm that the specimen coated at room temperature and plating time 20 minutes exhibited the highest corrosion resistance. Meanwhile, corrosion resistance of specimens coated at room temperature was better than those coated at 45^0 C. This can be caused from the releaseation of H_2 gas during the plating process lead to uneven crystal sizes with some defects in coatings. Electrochemical impedance spectroscopy (EIS) was also employed to investigate the corrosion resistance of A6063 substrate with and without coatings. Figure 4b displays the Nyquist impedance spectrum of the specimens. The determination of corrosion rate is associated with the charge transfer resistance (Rct) using EIS technique, where Rct is equal to the diameter of the semicircle in the Nyquist impedance spectrum. The overall increase in Zre of the specimens can be attributed to the formation of an inner passive layer. The Zre value for the A6063 substrate was $1.75x10^2$ ohm and the specimens coated at TR-20 min-, TR-40 min-, TR-60 min-, 45C-20 min-, 45C-40 min-, 45C-60 min-specimens, it was $2.17x10^3$, $1.03x10^3$, $7.42x10^2$, $2.74x\ 10^2$, $4.38x10^2$,and $5.52x10^2$ ohm, respectively. Notably, there was a significant increase in the Z' value for the TR-20 min- specimen. This increase in Zre values is attributed to the formation of the homogenous precipitated crystals arranged in a tile-roof stacked pattern on the A6063 substrate, which created a protective layer improving the corrosion resistance. Fig. 5. illustrates the polarization curves and EIS of the Au/Ni-coatings samples. The i_{corr} and E_{corr} value of Au-electroplating coating at different plating time and various temperature were calculated as follows: the i_{corr} values are 7.91, 1.92, 1.51, 5.12, 3.98 and 26.33 μA/cm² and E_{corr} values are -382, -293, -282, -401, -450 and -405 mV for Au-TR-20 min-, Au-TR-40min-, Au-TR-60min-, Au-45C-20min-, Au-45C-40min-, Au-45C-60min-specimens, respectively. These results show that the

https://doi.org/10.62239/jca.2024.067

corrosion resistance of A6063 was often enhanced by additing a Au-electroplating coating as compared to samples with only Ni-coated and far superior to those without coating. This is the result of the inner Ni layer and the outer gold layer's combined protective effect. In which, the corrosion protection of the gold layer is better than Ni layer due to the chemical inertness of gold in acidic environments and has been shown in previous study [19]. In particular, the corrosion current density of the Au/Ni coated sample is reduced by 6.4 times compared to the Ni-coated sample and 33.9 times compared to the A6063 sample without coating and achieved at electroplating parameter of room temparature and 60 minutes. Similar to Ni plating, the resultant coatings exhibited lower corrosion resistance when the plating bath temperature is increased to 45° C.

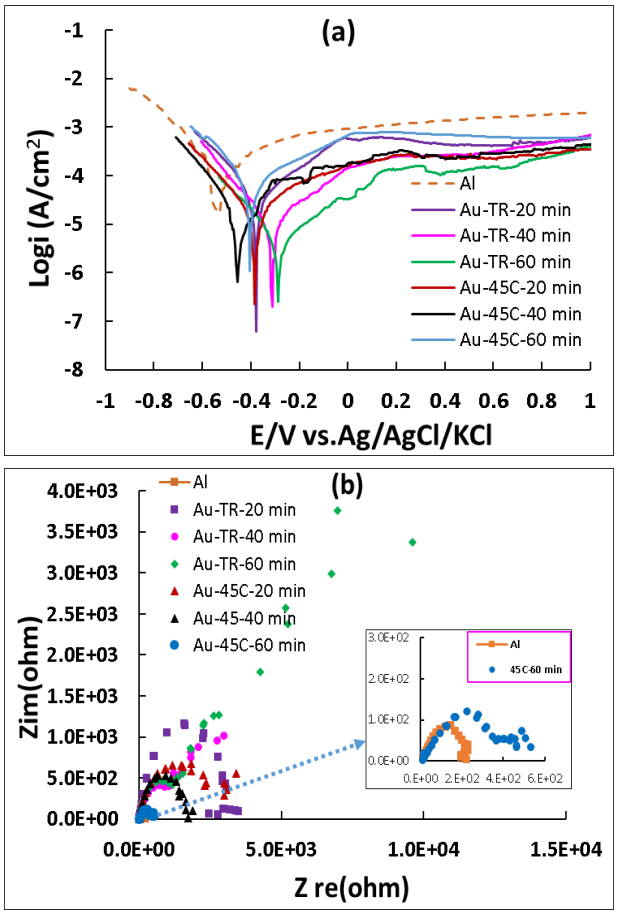

Fig. 5. (a) Polarization curves and (b) EIS of Au/Ni-coatings

Static corrosion behavior

After immersing samples in a solution of 0.5 M H_2SO_4 + 200 ppm HF at 60^0 C, the corrosion rate value of samples was caculated and shown in Fig 6. During 14 days of immersion, the corrosion rate is 0.020 mm/year for Ni-coating and 0.001 mm/year for Au/Ni-coating. The corrosion rate increased very rapidly in the period from 14 days to 30 days, then increased slightly in the case of Ni- coating. Meanwhile, the corrosion rate of Au/Ni-coating sample increased insignificantly during immersion until the end of the experiment. After 45 days immersion, the corrosion rate was 0.119 and 0.005 mm/year for Ni-coating and Au/Ni-coating samples, respectively. Those results in this experiment is smaller than that in Tafel extrapolation method from Polarization curves because electrochemical measurements accelerated by applying a voltage.

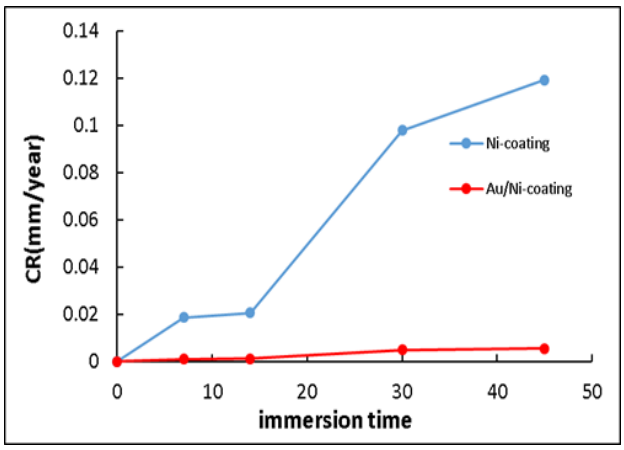

Fig 6. corrosion behavior with immersion time

Conclusion

Ni-coating and Au/Ni-coating were successfully prepared on Aluminum alloy A6063 by electroplating method. Ni-coating was performed at room temperature (25^0 C) and 45^0 C, cathode current density is 0.8 A/dm^2, pH of solution of 4 and various plating time of 20, 40, and 60 minutes, using a DC power source. While, Au/Ni-coating applied the samples which have a available intermediate Ni-coatings with electroplating time of 20 minutes, and continued Au-coated process in various time of 20 to 60 minutes, cathode current density is 0.6 A/dm^2. Aluminum alloy A6063 with protective coatings (Ni-coating and Au/Ni-coating) significantly improved the corrosion resistance than that compared to Aluminum alloy A6063 without protective coating in a simulated environment proton exchange membrane fuel. The Ni-coating at temperature of room temperature (25° C) and plating time of 20 minutes exhibited the highest corrosion resistance. Meanwhile, Au/Ni-coating has the best corrosion resistance at temperature of 25° C and plating time 60 minutes.

https://doi.org/10.62239/jca.2024.067

Acknowledgments

This research is funded by the Vietnam Academy of Science and Technology (VAST) under Grant number TĐHYD0.02/22-24.

References

1. Wei-Wei Yuan, Ou Kai, Young-Bae Kim, Appl. Therm. Eng 167 (2020) 114715. https://doi.org/10.1016/j.applthermaleng.2019.114715
2. F.G. Werner, L. Busemeyer, J. Kallo, S. Heitmann, M. Griebenow Werner et al,Int. J.Hydrogen Energy (2020) 1–19. https://doi.org/10.1007/S13272-014-0142-Z
3. Setareh Shahsavari, Andrew Desouza, Majid Bahrami, Erik Kjeang, Int. J.Hydrogen Energy 37 (2012) 18261–18271. https://doi.org/10.1016/j.ijhydene.2012.09.075
4. E. Middelman, W. Kout, B. Vogelaar, J. Lenssen, E. de Waal, J. Power Sources 118 (2003) 44–46. https://doi.org/10.1016/s0378-7753(03)00070-3
5. M. Marappan, K. Palaniswamy, T. Velumani, K. B. Chul, R. Velayutham, P. Shivakumar, S. Sundaram, Chem. Rec 21 (2021) 663–714. https://doi.org/10.1002/tcr.202000138
6. Magdalena Dudek, Andrzej Raźniak, Bartłomiej Lis, Michał Kawalec, Mariusz Krauz,Tadeusz Wójcik, E3S. Web. Conf 14 (2017) 01042. https://doi.org/10.1051/e3sconf/20171401042
7. Richard Stroman, Michael W. Schuette, Nav. Res 2010, 1–43. https://doi.org/10.21236/ada525161
8. J. Wu, S. Galli, I. Lagana, A. Pozio, G. Monteleone, X. Zi Yuan, J. Martin, H. Wang, J. Power Sources, 188 (2009) 199–204. https://doi.org/10.1016/j.jpowsour.2008.11.078
9. Chih-Yung Wen, Guo-Wei Huang, Res.Express 6 (2008) 1–8. https://doi.org/10.1016/j.jpowsour.2007.12.040
10. Ahn Jong-Woo and Choe, Song-Yu, J. Power Sources 179 (2008) 252–264. https://doi.org/10.1016/j.jpowsour.2007.12.066
11. F A. Fly , R.H. Thring, Int. J. Hydrogen Energy, 41 (2016) 14217–14229. https://doi.org/10.1016/j.ijhydene.2016.06.089
12. G. Zhang, S.G. Kandlikar, Int. J. Hydrogen Energy 37 (2012) 2412-2429. https://doi.org/10.1016/j.ijhydene.2011.11.010
13. Q. Li, Z. Liu ,Y. Sun, S. Yang, C. Deng, Processes, 9(2) (2021) 235. https://doi.org/10.3390/pr9020235
14. Comparini, Andrea Del Pace, Ivan Giurlani, Walter Emanuele, Roberta Verrucchi, Margherita Bonechi, Marco Innocenti, Massimo, Coatings, 13(1) (2022) 13. https://doi.org/10.3390/coatings13010013
15. L. Aydi, M. Khli, C. Bradai, S. Spigarelli, M. Cabibbo, M. El Mehtedi, Materials Today: Proceedings, 2(10) (2015) 4890-4897. https://doi.org/10.1016/j.matpr.2015.10.044
16. André Ribeiro Morais, Electroplated Ni-Al_2O_3 nanocomposite coatings on aluminium alloys. Master's degree dissertation of metalurgical and material engineering at Faculty of Engineering of University of Porto (2022).
17. Hue N.V, Phong N.N, Tuyet N.T.A, Met Mater Int, 12(6) (2006) 493-496. https://doi.org/10.1007/BF03027749
18. Hue N.V, Tuyet N.T.A, Hanh P.H, Phong N.N, Trans. Nonferrous Met. Soc. China, 23 (2013) 2348–2353. https://doi.org/10.1016/S1003-6326(13)62740-5
19. Rautio T, Hamidreza T, Tarek A, Antti J, Atef H, Mater. Res. Technol, 17 (2022), 521–536. https://doi.org/10.1016/j.jmrt.2022.01.022